Enhancing 5G and 6G Communication with Tripartite Perfect W-States and LOCC Approach

Mansoor A. Khan[1], *Member, IEEE*, Muhammad N. Aman[2*], *Senior Member, IEEE*, and Biplab Sikdar[1], *Senior Member, IEEE*

[1]Department of Electrical and Computer Engineering, National University of Singapore, 117575, Singapore (e-mail: dr.mak@nus.edu.sg, bsikdar@nus.edu.sg)
[2]School of Computing, College of Engineering, University of Nebraska, Lincoln, NE 68588, United States (e-mail: naveed.aman@unl.edu)
*Corresponding author: Muhammad N. Aman (e-mail: naveed.aman@unl.edu).

This work is supported by the National Research Foundation, Singapore and A*STAR under its Quantum Engineering Programme (National QuantumSafe Network, NRF2021-QEP2-04-P01).

***Abstract*—**The rapid evolution of communication networks to 5G/6G has introduced significant challenges, particularly in ensuring data security, low latency, high throughput, efficient energy consumption, dynamic access to multiple connection types, and managing the influx of connected devices. Quantum communication, leveraging entangled states like the perfect W-state, offers a promising solution with its high degree of entanglement, secure information transmission, and resilience against decoherence. However, practical applications and experimental validations remain limited, especially regarding the integration with Local Operations and Classical Communication (LOCC) protocols. Additionally, optimizing perfect W-state-based communication protocols for the splitting and sharing of quantum information has been scarcely explored. This article presents a Quantum Information Sharing and Splitting (QISS) protocol that integrates perfect W-states with LOCC to enhance 5G and 6G communication. Using the Eagle r3 processor based on superconducting qubits, our experiments demonstrated a fidelity of 0.82 ± 0.02 for the perfect W-state circuit and 0.55 ± 0.03 for the integrated W-state + LOCC in the QISS communication prototype. These findings, quantified through quantum state tomography, significantly improve communication security, network densification, and effectiveness. Furthermore, our research addresses existing gaps in quantum communication implementation, paving the way for scalable quantum networks and advanced encryption methods. This work marks a substantial step towards secure and efficient data transmission in next-generation communication systems.

I. Introduction

The rapid transition to 6G communication represents a remarkable journey of technological advancements. Each generation of mobile communication has brought unprecedented improvements in data speeds, capacity, functionality, and connectivity [1]. For instance, 2G marked the shift from analog to digital communication networks, providing basic digital voice services and text messaging with data bandwidth up to ~64kbps. 3G networks introduced higher data rates (up to ~2 Mbps) and the ability to support multimedia applications, paving the way for mobile internet access [2]. 4G networks delivered even faster data speeds (exceeding 100+ Mbps) and improved internet connectivity, enabling high-definition video streaming and more robust mobile applications. Emerging 5G networks promise ultra-fast data speeds (~1-10 Gbps), low latency, and the capability to connect a massive number of devices, which are essential for IoT, smart cities, and real-time applications [3]. Until now, 5G commercial networks have been launched in over 60 countries. The successor to 5G cellular technology, 6G networks, still in the research phase, are anticipated to deliver unprecedented data rates (at least 1 Tbps), near-zero latency, and advanced applications such as holographic communications and integrated AI-driven services [4]. However, these advancements come with significant challenges. For 5G and 6G networks, key issues include ensuring data security, scalability to manage the massive increase in connected devices, maintaining low latency over vast distances, and meeting various quality of service (QoS) requirements [5], [6]. Traditional cryptographic methods may not suffice to address these challenges, necessitating the exploration of quantum communication techniques.

In recent years, quantum communication has gained significant attention as a secure way of transferring data, leveraging quantum superposition and entanglement [7], [8]. Superposition enables more efficient information processing, while entanglement ensures the security and integrity of transmitted data, quantum communication protocols, such as Quantum Key Distribution (QKD), use entangled states to securely exchange encryption keys encoded in quantum states using qubits [9]. Notable implementations include China's Micius satellite, the world's first quantum communication satellite for entanglement-based QKD [10], and Quantum Xchange's planned 500-mile Phio network in the U.S., the first commercial QKD network [11]. Toshiba has also successfully demonstrated QKD transmission over a 600-kilometer optical fiber network [12], and China Telecom has piloted quantum-encrypted VoIP calls using specialized SIM cards. In 2020, Samsung and SK Telecom launched the Samsung *Galaxy A Quantum*, the first 5G phone featuring quantum encryption [13].

In quantum communication, the tripartite entangled W-state, composed of three qubits, is extensively researched for its robust entanglement and resistance to decoherence, setting it apart from other entangled states [14], [15]. W-states have applications in quantum communication protocols like QKD, quantum teleportation, quantum error correction, superdense coding, and measurement-based quantum computing (MBQC) techniques [16], [17]. Despite the promise of quantum communication, experimental validation and practical implementation of quantum protocols using entangled states like perfect W-states remain limited. Furthermore, the integration of these states with Local Operations and Classical Communication (LOCC) to enhance communication efficiency and security has not been extensively explored.

This manuscript addresses existing gaps by introducing a new prototype that integrates tripartite perfect W-states with LOCC. We propose a Quantum Information Sharing and Splitting (QISS) protocol, utilizing the high degree of entanglement and decoherence resilience of perfect W-states.

Our experiments using superconducting qubits demonstrate significant improvements in fidelity and security. This synergy enhances the effectiveness of quantum communication systems, making it a viable solution for 5G and 6G challenges. Key contributions include:

i. Development of the QISS protocol, enabling the creation and control of W-states via LOCC.

ii. Optimization of perfect W-states with LOCC for enhanced security and efficiency in quantum communication.

iii. Measurement of prototype performance using quantum state tomography, with experimental results demonstrating high fidelity in perfect W-state circuits and integrated perfect W-state and LOCC systems.

iv. By providing both theoretical and experimental evidence, this research addresses gaps in classical and quantum communication, laying the foundation for future scalable quantum networks that ensure secure 5G and 6G communication. This work advances the practical implementation of these protocols in next-generation mobile networks, enabling robust data transmission.

This paper is organized as follows: Section II discusses quantum entanglement and compares its key classes. Section III provides a detailed overview of the perfect W-state, LOCC, and the QISS communication prototype, along with simulations, experimental results, and illustrative examples. Section IV analyzes the benefits and performance. Finally, Section V concludes the paper.

II. Background

A. *Manifestations of Quantum Entanglement*

Quantum physics, fundamentally probabilistic, introduces superposition and entanglement, which are pivotal for achieving *Quantum Supremacy*— where quantum computers surpass classical one [18]. For instance, Shor's algorithm factors integers in $O((\log N)^3)$ time, posing a potential to break RSA encryption in polynomial time, while Grover's algorithm offers a quadratic speedup to $O(\sqrt{N})$ time for searching unsorted data, outperforming classical $O(N)$ algorithms [19].

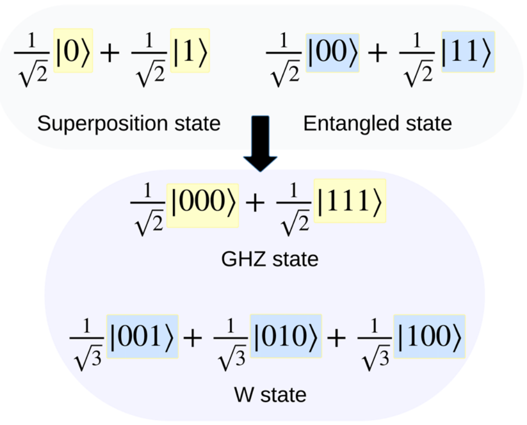

(a) Quantum notation for bipartite and tripartite states.

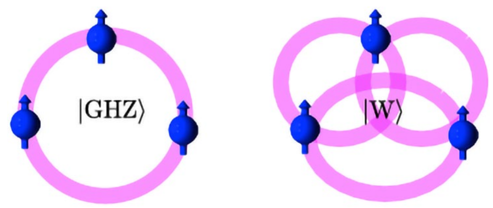

(b) GHZ vs W-class state entanglement.

Fig. 1 (a) Comparison of entanglement categories, **(b)** Illuminating the Quantum dance to differentiate GHZ vs. W-Class entangled states.

Entanglement, a cornerstone of quantum computing, underpins secure quantum cryptography, enables quantum teleportation over long distances, and is essential for large-scale quantum networks and distributed quantum computation. It also enables efficient simulation of complex quantum systems, driving advancements in fields like machine learning, AI, drug discovery, materials science, and finance, which are challenging for classical computation. Entanglement can be bipartite, as in Bell states, or multipartite, as in Greenberger-Horne-Zeilinger (GHZ) and W-states [14], [20], as summarized in Table I. GHZ states exhibit genuine tripartite entanglement, while W-states are

Table I. Comparative analysis of entanglement types.

Attribute	Bipartite	GHZ	W-state
Degree of Entanglement [21]	Two qubits	Three qubits	Three qubits
Basis of Construction [15]	Bell states/EPR pairs	Maximally entangled Multi-qubit state	Symmetric state that can be created from high-degree multipartite entangled pairs
Key Feature [14]	Classical correlation and entanglement.	Genuine multipartite entanglement among all qubits.	High-degree of multipartite entanglement and robustness to noise
Robustness to Decoherence [18] [21]	Vulnerable to decoherence in long-distance channels	Sensitive to noise	Resilient against certain types of decoherence
Mathematical Form (s) [20]	$\lvert\Phi^+\rangle = \frac{1}{\sqrt{2}}(\lvert 00\rangle + \lvert 11\rangle)$ $\lvert\Phi^-\rangle = \frac{1}{\sqrt{2}}(\lvert 00\rangle - \lvert 11\rangle)$ $\lvert\Psi^+\rangle = \frac{1}{\sqrt{2}}(\lvert 01\rangle + \lvert 10\rangle)$ $\lvert\Psi^-\rangle = \frac{1}{\sqrt{2}}(\lvert 01\rangle - \lvert 10\rangle)$	$\lvert GHZ3\rangle = \frac{\lvert 000\rangle}{\sqrt{2}} + \frac{\lvert 111\rangle}{\sqrt{2}}$	$\lvert W3\rangle = \frac{\lvert 001\rangle}{\sqrt{3}} + \frac{\lvert 010\rangle}{\sqrt{3}} + \frac{\lvert 100\rangle}{\sqrt{3}}$ $\lvert W_P\rangle = \frac{1}{2}(\lvert 100\rangle + \lvert 010\rangle + \sqrt{2}\lvert 001\rangle)$
Robustness against particle loss [7] [9]	Decreases with particle loss	Becomes fully separable after losing one qubit	Remains entangled after losing one qubit.

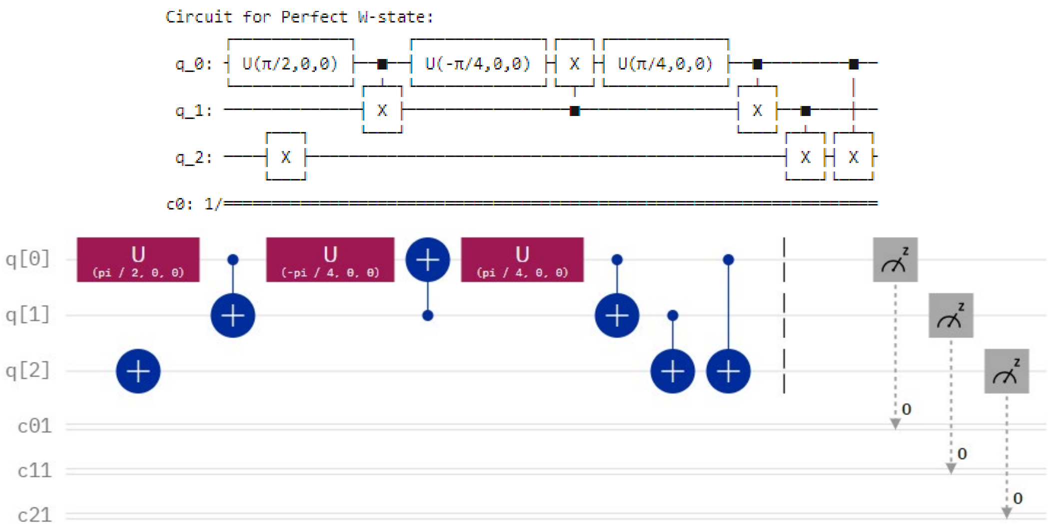

(a) Schematic illustrations of Quantum Circuit to generate perfect W-state

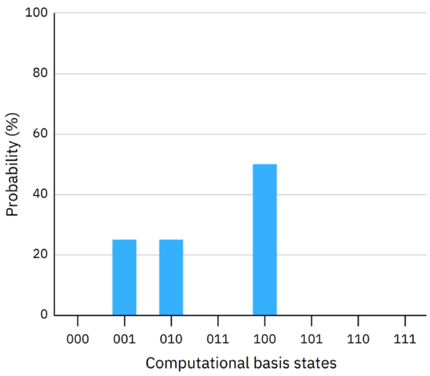

(b) Probabilities histogram.

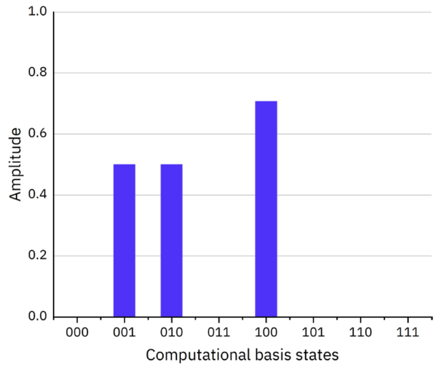

(c) Statevector histogram.

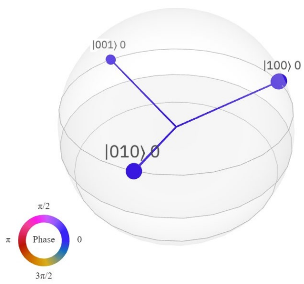

(d) Q-sphere with phases.

Fig. 2. Simulation results of the generated perfect W-state, showing quantum information mapping and analysis.

notable distinguished by its robustness and unique entanglement characteristics. These states are crucial in quantum applications like quantum secret sharing, quantum teleportation, QKD, quantum dense coding, and quantum error correction, They enable secure cryptography, efficient information processing, and robust quantum communication, facilitating advances in diverse fields.

B. *The Quest for W-Class State Tripartite Entanglement*

To delve into this quest, it's vital to understand that tripartite entanglement plays a fundamental role in quantum information theory (QIT). Among the most prominent forms of this entanglement are the GHZ and W states, which differ in how their qubits are entangled. In a GHZ-state, *all three qubits* are mutually entangled, with each qubit's state dependent on the others (Fig. 1a). In contrast, in a W-state only *two* of the three qubits are directly entangled, while the third qubit is entangled with the combined state (product) of the other two (Fig. 1b). This configuration gives W-states a unique advantage in resilience against decoherence, allowing them to maintain entanglement for longer periods than GHZ states [21]. The distinction between these states becomes most apparent when measuring the third qubit, as emphasized in Table I. For example, if the measurement outcome is 0, the three qubits of the GHZ-state collapse to $|000\rangle$, whereas the W state collapses to $\frac{|010\rangle}{\sqrt{2}}+\frac{|100\rangle}{\sqrt{2}}$, with the remaining qubits forming a maximally entangled Bell state, known as pairwise entanglement (Fig. 1b). Similarly, if the first qubit in a W-state is measured and results in 1, the state collapses to $|100\rangle$. This demonstrates that W-states retain strong entanglement properties even when a qubit is lost, in contrast to GHZ states. These distinct types of entanglement, each with its unique strengths and weaknesses, showcase a range of fascinating properties.

III. Experimental Generation of W-state via Quantum Circuits

In this work, we utilized the IBM Quantum Qiskit SDK and the 127-qubit Eagle r3 quantum processor with superconducting qubits (SQs) to simulate and experimentally generate W-state quantum circuits, including a tripartite W-state and LOCC prototype. IBM's quantum computing via the SQs platform marks a pivotal advancement in the field of quantum physics research, as it is highly effective at very low temperatures and exhibits coherence times between 100 and 300 µs. For instance, the 'ibm_osaka' Eagle r3 processor typically has a median coherence time (T2) of around 169.88 µs, while newer materials used in processors like the Falcon r8 can achieve coherence times greater than 0.3 ms (~320 µs). The SQs platform has been instrumental in a variety of proof-of-concept experiments, including those that test Bell's inequalities to validate the concept of quantum entanglement, design quantum routers, enable dense coding, study the behavior of magnetic materials, and confirm the no-hiding theorem. Furthermore, this platform has supported quantum

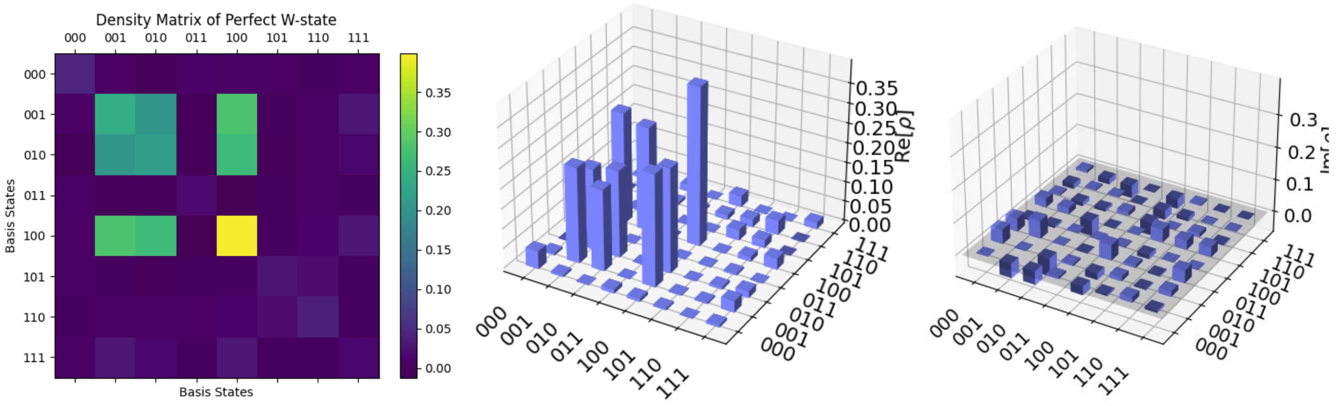

(a) 2D plot of density matrix **(b)** 3D plot of density matrix (real part) **(c)** 3D plot of density matrix (imaginary part).

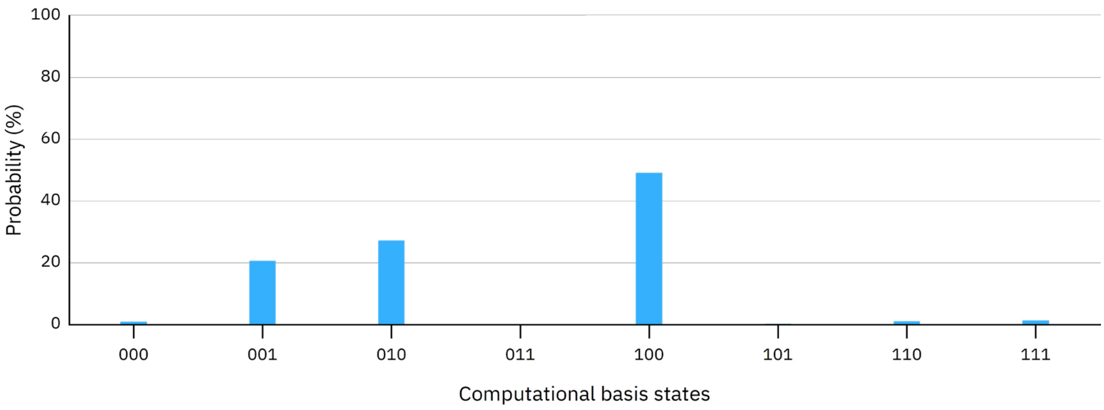

(d) Probabilities histogram.

Fig. 3. Experimental results of the generated Perfect W-State using IBM 'ibm_osaka' Eagle r3 processor (8192 shots).

simulations, the implementation of Shor's algorithm, quantum cheque transactions, quantum secret sharing, and quantum error correction. These extensive applications demonstrate the platform's vital role in pushing the frontiers of quantum physics research [22].

To experimentally realize our protocol, we initially generated maximally entangled tripartite W-states qubits, holding uniformly distributed probabilities (~33%) and amplitude values (~ 0.57 or $1/\sqrt{3}$), validating Eq. (1).

$$|W3\rangle = \frac{|001\rangle}{\sqrt{3}} + \frac{|010\rangle}{\sqrt{3}} + \frac{|100\rangle}{\sqrt{3}}. \quad (1)$$

Eq. (1) is derived from the general expression of a W-state, given as [23], [24]:

$$|W\rangle = \sum_i p_i |1_i, \{0\}\rangle,$$
$$\sum_i |p_i|^2 = 1, \quad (2)$$

and where p_i denotes the probability amplitudes, and the state $|1_i, \{0\}\rangle$ indicates the i-th qubit being in the '1' state while all others are in the '0' state. The condition $\sum |p_i|^2 = 1$ ensures the state is normalized, i.e., the total probability sums to 1. When p_i is set to $1/\sqrt{N}$ (where N is the number of qubits), the state becomes a uniformly distributed:

$$|W\rangle = \frac{1}{\sqrt{N}}(|100..0\rangle + |010 \dots 0\rangle\rangle + \cdots + |0..001\rangle), \quad (3)$$

Eq. (1) reflects a special case of Eq. (3) where all the amplitudes are equal, representing a maximally entangled W-state. However, it is important to highlight there is another category of W-stated called that "perfect" W-state. The primary distinction lies in the "weights and phases" of the terms within the state. Using the Eq. (3), we can derive the general mathematical form of a tripartite (3-qubit) perfect W-state as follows:

$$|W_{p,s}\rangle = \frac{1}{\sqrt{2+2s}}\left(|100\rangle + \sqrt{s}e^{i\Phi_1}|010\rangle + \sqrt{s+1}e^{i\Phi_2}|001\rangle\right), \quad (4)$$

where s is a real number that scales the amplitudes, and Φ_1, Φ_2 are phases associated with the terms. The normalization factor $\frac{1}{\sqrt{2+2s}}$ ensures that the total probability sums to 1. If we If we set $s = 1$ and $\Phi_1 = \Phi_2 = 0$, then Eq. (4) becomes:

$$|W_p\rangle = \frac{1}{2}(|100\rangle + |010\rangle + \sqrt{2}|001\rangle). \quad (5)$$

Contrary to maximally entangled states (Eq. (1)), the perfect W-state (Eq. (5)) differs in the coefficients and phases of its constituent terms, deviating from the standard characteristics of a maximally entangled W-state. The presence of $\sqrt{2}$ indicates a different weight for the amplitude associated with the $|001\rangle$ state. We generated and evaluated the perfect

W-state as described in Eq. (5) using IBM's 'ibm_osaka' for 8192 shots, as demonstrated in Fig. 2. The simulated and experimental results are shown in Figs. 2 and 3. Statistical analysis reveals the states differ slightly in terms of weights, as reflected in the probability histogram (Fig. 2b) and amplitude by the state vector histogram (Fig. 2c). However, the phases remain identical, as depicted in the Q-sphere plot (Fig. 2d), aligning with the characteristics of the perfect W-state described in Eq. (5). This indicates that, unlike the maximally entangled W-state, the perfect W-state is meticulously engineered with precise control over the coefficients and phases of its constituent terms, rendering it exceptionally well-suited for a variety of applications. The capacity to precisely manipulate the phase and amplitude (weights) of the components in a perfect W-state presents substantial advantages in quantum information processing, including the following:

1) Benefits of Changing the Phase

- *Interference Control:* Modifying the phase can adjust the interference pattern in quantum algorithms, enabling precise result fine-tuning. For example, in quantum teleportation protocols that depend on specific interference patterns, phase adjustments can enhance the fidelity of the teleported state.
- *Quantum Communication:* In protocols such as QKD and quantum information sharing, phase adjustments can improve security by making the state less predictable.
- *State Discrimination:* Varying the phases can enhance the distinguishability of states, which is essential in quantum measurement and state discrimination tasks. For instance, in quantum cryptography, altering the phase can make quantum states more resistant to eavesdropping, as the eavesdropper must correctly determine the phase to access the information.

2) Benefits of Changing the Amplitude

- *Robustness to Loss:* Tuning amplitudes can enhance the robustness of a quantum state against qubit loss. In a standard tripartite W-state $\frac{1}{\sqrt{3}}(|001\rangle + |010\rangle + |100\rangle)$, equal amplitudes signify symmetric entanglement among the three qubits. However, when the amplitudes are varied, as in a modified W-state $a|001\rangle + b|010\rangle + c|100\rangle$, where a, b, c are complex numbers with $|a|^2 + |b|^2 + |c|^2 = 1$, the distribution of entanglement becomes asymmetric. This asymmetry can be advantageous if one qubit is more prone to loss or corruption. For example, if the qubit associated with the $|001\rangle$ state is more likely to be lost, setting the amplitude a smaller than b and c reduces the overall state's dependency on that qubit. As a result, even if that qubit is lost, the remaining qubits, with their larger amplitudes, maintain substantial entanglement, thereby preserving the integrity of the quantum state. This strategy of tuning amplitudes helps anticipate and mitigate potential losses, making the quantum state more robust for practical applications in quantum communication and computing.
- *Entanglement Distribution:* Adjusting amplitudes can control how entanglement is distributed among the qubits, which is useful in quantum networking.
- *State Preparation:* Varying amplitudes allows for the preparation of states tailored to specific tasks in quantum communication and computation.

3) Quantum Tomography and Fidelity

To evaluate the quality of the generated perfect W-state, we conducted a comprehensive quantum state tomography (QST) and calculated the state fidelity, as shown in Fig. 3. QST is a highly effective tool that gathers comprehensive information about the quantum state by conducting complementary measurements, rather than relying solely on $|Z\rangle$-basis measurements. This series of measurements allows us to reconstruct the density matrix of the quantum state. In quantum information, it is often necessary to compare two density matrices to quantify their similarity or difference. QST is used to evaluate the accuracy of quantum state preparation by comparing the experimentally reconstructed density matrix ρ with the theoretical or target density matrix σ. This comparison is made using a metric called quantum fidelity, which is a fundamental figure of merit in quantum state analysis. Fidelity measures how closely the experimentally obtained state matches the ideal state. The fidelity (F) of two quantum states, represented by their density matrices ρ and σ, is expressed as:

$$F(\rho, \sigma) = \left\{ \mathrm{Tr} \left(\sqrt{\sqrt{\rho}\sigma\sqrt{\rho}} \right) \right\}^2, \qquad (6)$$

where Tr denotes the trace of a matrix, which is the sum of all its diagonal elements. The square root of a density matrix is defined via its eigen decomposition. For the special case where one of the states is a pure state, say $\sigma = |\psi\rangle\langle\psi|$), the fidelity simplifies to:

$$F(\rho, |\psi\rangle) = \langle\psi|\rho|\psi\rangle \ . \qquad (7)$$

This represents the probability that the state ρ will pass a test to be identified as the state $|\psi\rangle$.

In our QST analysis, we reconstructed the density matrix ρ experimentally and then calculated the fidelity to assess how well the reconstruction matches the expected theoretical state σ. This analysis provides insight into the accuracy of the quantum W-state preparation and measurement processes, thereby validating the effectiveness of our approach. In Figs. 3a-c, the 2D and 3D density matrix plots illustrate that the diagonal elements, ranging from '000' to '111', represent the probabilities of the system being in each respective basis state. In Fig. 3a, the 2D color-coded density matrix depicts the quantum system's state, encompassing both pure and mixed states. The off-diagonal elements signify the coherence terms, which are vital in quantum mechanics for conveying information about the superposition and entanglement of states. Bright squares in the matrix indicate higher probabilities or coherences, highlighting the superposition and entanglement of the involved qubits. From these plots, it is evident that in a perfect W-state for a three-qubit system, the density matrix should ideally display non-zero elements (as indicated by green and yellow squares) exclusively at positions '001', '010', and '100'. The coherences among these states, specifically ('001', '010'), ('001', '100'), and ('010', '100'), confirm the entanglement characteristic of the W-class quantum system, as shown in Eq. (5) and Fig. 1b.

The 3D histograms in Figs. 3b-c demonstrate both the real and imaginary parts of the density matrix elements, providing a visual representation of the quantum state's structure and

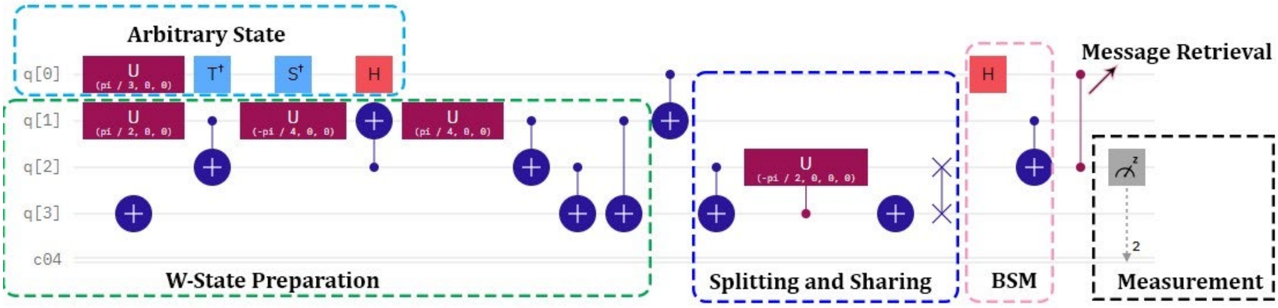

(a) Schematic illustration of QISS prototype using quantum circuits for generating perfect W-state with LOCC.

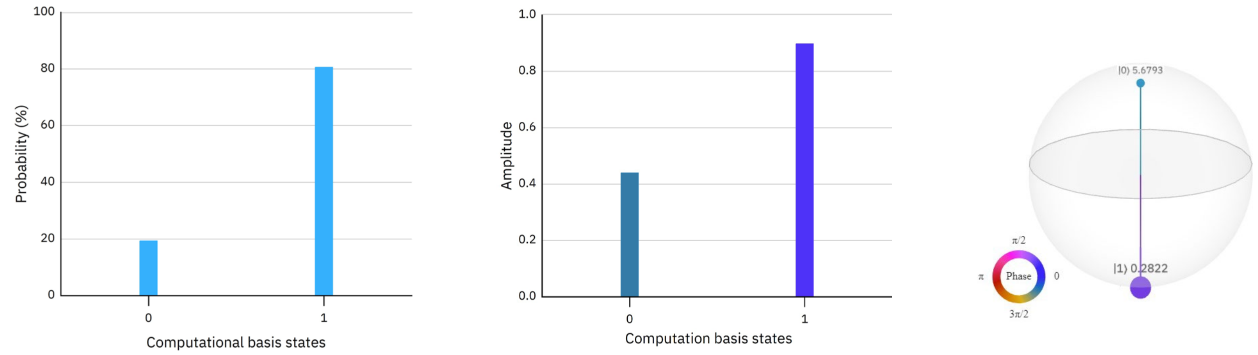

(b) Arbitrary state preparation by sequence of single-qubit quantum gates with probabilities, statevector histograms, and Q-sphere with phases.

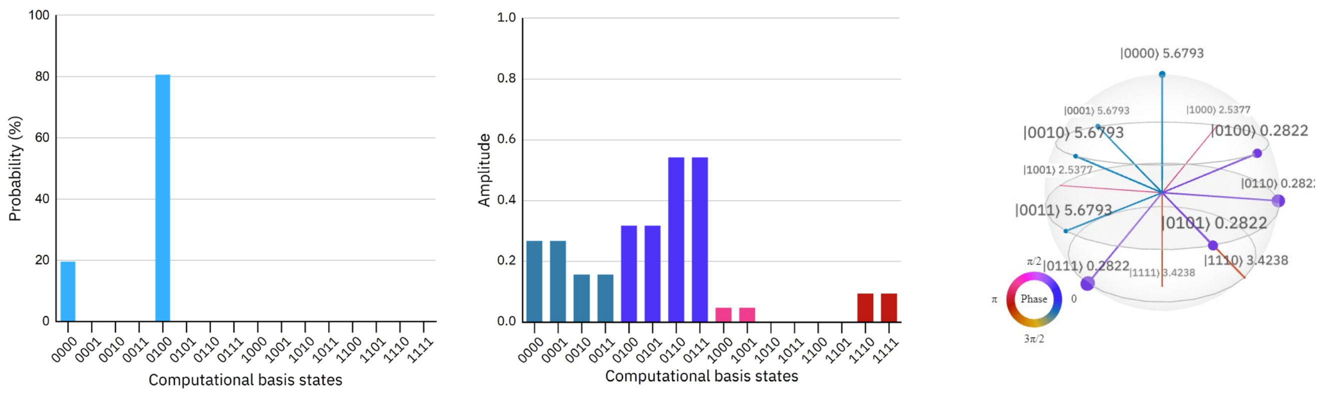

(c) Probabilities histogram (Bob's receiver qubit). **(d)** Statevector histogram (all qubits) **(e)** Q-sphere with phases.

Fig. 4. Simulation results: Quantum information mapping and analysis of QISS communication process.

dynamics. In the real part plot, each bar's height reflects the magnitude of the real components, where significant bars suggest stronger contributions from those basis pairs—particularly important in a W-state where notable peaks highlight substantial multi-qubit states. Similarly, the imaginary part plot underscores the phase relationships between components, with non-zero values indicating essential superpositions and entanglements that underpin quantum computation and information protocols. Additionally, the simulated probabilities histogram (Fig. 2b) and the experimentally measured probabilities histogram (Fig. 3d) corroborate the weights and phases detailed in Eq. (5). Furthermore, the results reveal that the fidelity of the generated perfect W-state circuit is approximately 0.82 ± 0.02, indicating that the experimental state closely resembles the perfect W-state but shows slight imperfections, likely due to errors or noise in the SQs or quantum circuits.

In the next section, as part of quantum information theory (QIT), we aim to distill or enhance the entanglement of the given state by using the LOCC paradigm to perform local measurements instead of non-local or global operations [25].

IV. Prototype of Perfect W-state using LOCC for QISS Communication

Unlike quantum teleportation, a one-way protocol, LOCC protocols are two-way, enabling joint operations on shared entangled states like W-states or GHZ-states. LOCC can transition from two-qubit to three-qubit states, with W-states preferred for their more robust entanglement. Additionally, the capability to adjust phases and amplitudes in perfect W-states enables more sophisticated manipulation and control of quantum states. In this paper, we empirically implement the QISS scheme integrated with LOCC prototype using a perfect W-state shared among three parties Alice, Bob, and Charlie (Fig. 4). The process flow is as follows:

1) **Initial State:** The three parties initially share an entangled W-state:
$$|W\rangle = \frac{1}{2}\left(|0_A 0_B 1_C\rangle + |0_A 1_B 0_C\rangle + \sqrt{2}|1_A 0_B 0_C\rangle\right) \quad (8)$$

2) **Information Qubit:** Alice has an information qubit (q_0):
$$|\phi_i\rangle = \alpha|0_i\rangle + \beta|1_i\rangle. \quad (9)$$

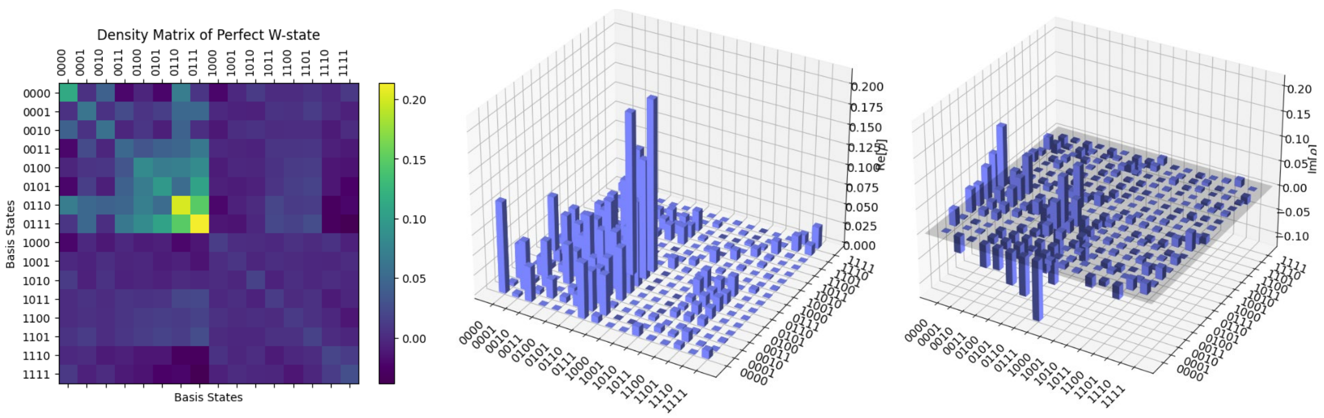

(a) 2D plot of density matrix **(b)** 3D plot of density matrix (real part) **(c)** 3D plot of density matrix (imaginary part).

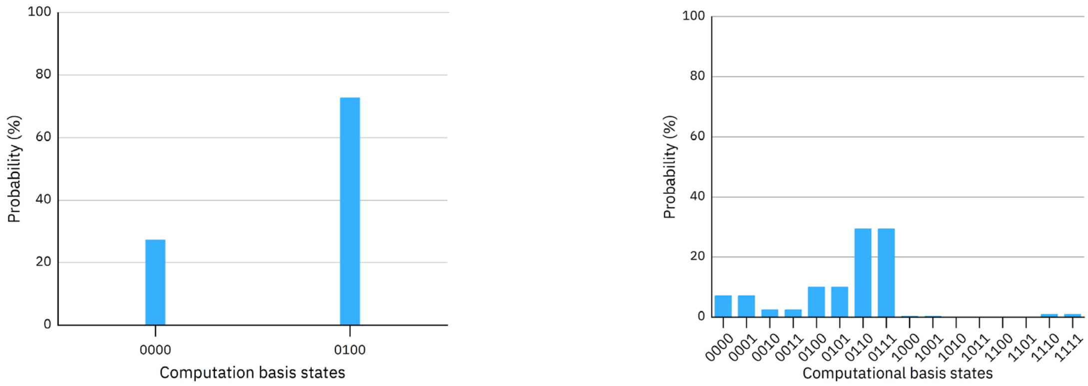

(e) Probabilities histogram (Bob's receiver qubit) **(d)** Probabilities histogram (all qubits).

Fig. 5. Experimental results: Quantum information mapping and analysis of QISS communication process—IBM 'ibm_osaka' Eagle r3 processor (8192 shots).

The composite state is expressed by the tensor product of the W-state and Alice's information qubit:

$$|\Psi\rangle = \frac{1}{2}\alpha\left(|0_i 0_A 0_B 1_C\rangle + |0_i 0_A 1_B 0_C\rangle + \sqrt{2}|0_i 1_A 0_B 0_C\rangle\right) + \frac{1}{2}\beta\left(|1_i 0_A 0_B 1_C\rangle + |1_i 0_A 1_B 0_C\rangle + \sqrt{2}|1_i 1_A 0_B 0_C\rangle\right). \tag{10}$$

3) **Qubit Manipulation:** Alice manipulates her information qubit using single-qubit gates, such as $U3(\pi/3,0,0), Y, S_y$, and H, to generate an arbitrary state, as shown in Fig. 4a. Statistical data for qubit q_0, including probability profile, statevector histograms, and Q-sphere plots, are detailed in Fig. 4b.

4) **Bell-State Measurement (BSM):** Alice performs a BSM on her two qubits as part of the LOCC operation. The Bell states are denoted as $|\Phi^{\pm}\rangle$and $|\Psi^{\pm}\rangle$. The local operations, which can be any single-qubit unitary operations, allow Alice, Bob, and Charlie to independently manipulate their qubits. The possible unitary operations include *I* (identity), Pauli *X* (NOT gate), *Y* (bit and phase-flip gate), and *Z* (phase-flip gate).

5) **Classical Communication:** The BSM outcomes are shared with each other using classical communication (phone/internet), e.g., if the outcome is $|\Phi^{+}\rangle$, then the shared state is now a combination of $|00\rangle$ and $|11\rangle$. As Alice performs a BSM on her two qubits, this message can be received by either Bob or Charlie. But neither Bob or Charlie can retrieve the information alone, they must coordinate with each other.

6) **Quantum Information Splitting:** Bob and Charlie use LOCC to split and share the quantum information, with Charlie as the controller and Bob as the receiver. Bob performs a two-particle unitary transformation on qubits q_2 and q_3 to split the quantum information. The unitary operator projects Charlie's qubit to state $|0\rangle$, and the message signal is transferred to Bob.

7) **Information Retrieval:** Finally, Bob retrieves the message by applying a *CZ*-gate or Pauli *X* to his qubit, as shown in Fig. 4a. The simulated and experimental probability histograms for Bob's qubit (q_2) are shown in Fig. 4c and Fig. 5e, respectively. Figs. 4d-e and Fig. 5d facilitate the understanding and visualization of the states/forms of the other measured qubits. Figs. 5a and 5d correlate to indicate that states '0110', '0111' exhibit non-zero elements (yellow squares), where the state components overlap. This demonstrates correlations or entanglement between these particular states. Their phase relationship is indicated in the Q-sphere (Fig. 4e), while the 3D plot in Fig. 5c shows that they share the same phase.

8) **Communication Process and Information Splitting:** The entire communication process involves splitting quantum information using LOCC via a prepared perfect

W-state. In general, LOCC elements are embedded in steps 4 and 5, where Alice performs a BSM, and subsequently, Bob and Charlie engage in collaborative operations. The BSM is considered a form of LOCC operation because it involves measurements performed on qubits that are locally controlled by a party (Alice, in this case). The classical communication of BSM outcomes is essential for coordinating subsequent operations. The choice of operations depends on the classical information received, making it a key element in the LOCC protocol. Sharing and splitting of information occurs in steps 6 and 7, where Bob and Charlie collaborate to distribute the information asymmetrically. The entire communication process, i.e., integration of QISS and LOCC using W-state is summarized in Fig. 4a.

9) **QST and Fidelity:** The QISS communication prototype's simulated and experimental results include probability distribution graphs, statevector histograms, Q-sphere plots, and density matrices (Figs. 4 and 5). The overall fidelity is 0.55 ± 0.03, with imperfections likely due to errors or noise in the SQs quantum system and circuits.

In summary, this protocol combines quantum information splitting and local operations with classical communication, using perfect W-states to distribute quantum information in 5G and 6G networks. Parties perform local operations in their network entities, such as MSC/HLR/VLR, and share measurement outcomes via a classical channel.

V. Benefits of Integrating LOCC and W-States for QISS Communication

A. Secure against Adversarial Attacks

Any eavesdropper attempting to intercept entangled states will cause the quantum system to collapse, alerting the involved parties to the intrusion. This security feature is due to:

i. Entanglement relies on superposition, as it correlates the quantum states of two or more systems. Superposition is necessary because, until measured, the properties of quantum systems in superposition remain undefined [20].

ii. Superposition is fragile, making entanglement inherently subtle and delicate. This delicacy makes entangled states easily disturbed by external influences [26].

iii. Entangled states carry quantum information and therefore must exist in a superposition state. In an entangled pair or trio, no qubit has a definite state on its own; instead, the entangled qubits must be considered as a single, unified system rather than two or three separate entities.

iv. One of the most remarkable aspects of two- or three-qubit entanglement is that the qubits can only be strongly correlated with each other, and not with any other qubit—a concept known as the *monogamy of entanglement*. This means that if you and the person you want to communicate with already share entangled qubits, the quantum information cannot be correlated with any other qubits anywhere in the universe. This unique property makes the distribution of entanglement the backbone of a future quantum internet.

v. Another fascinating aspect of quantum systems is the 'No-Cloning' theorem, which asserts that qubits cannot be copied or cloned [27]. Consequently, a 'quantum photocopier' for duplicating qubits does not exist. However, it's important to note that while digital information encoded in qubits can be copied, a device capable of copying arbitrary qubits has not yet been developed [28].

B. Entanglement Distillation from W-States

W-states are multi-qubit entangled states where one qubit is entangled with others. Distilling entanglement from W-states is a challenge similar to extracting entanglement from mixed states. LOCC protocols play a crucial role in this process by performing local operations on the W-state qubits and using classical communication to refine the entanglement [25].

C. W-State as an Initial Resource

A three-qubit W-state serves as a valuable initial resource. With LOCC, parties like Alice, Bob, and Charlie can manipulate their qubits using local operations, apply gates, perform measurements, and communicate to transform the W-state. They can extract or enhance useful entanglement. The simplicity of creating robust W-states with available quantum resources, their resistance to noise, and their ability to sustain entanglement in noisy environments make them highly efficient for quantum communication systems.

D. Reduced Complexity

LOCC protocols typically require only local operations on W-states and classical communication, which reduces complexity compared to physically transmitting qubits over a quantum channel. These operations focus on distilling and reshaping the entanglement within the state for the desired application.

E. Higher Flexibility and Scalability

LOCC allows the exchange of classical information among the involved parties (e.g., Alice, Bob, and Charlie), enabling them to coordinate their local operations and adapt to the specific properties of the W-state for various entanglement-related tasks. Because LOCC protocols don't rely on a shared quantum channel, scaling to larger numbers of parties is easier, and they can be adapted to different types of physical communication channels. Contrary to non-local operations, LOCC protocols do not require highly specialized hardware for sending and receiving qubits, making their implementation potentially less expensive than that of quantum channels.

F. Higher Fidelity

LOCC protocols can be more reliable than quantum channels, particularly as the latter are still in their early development stages. The maturity of classical communication allows for error correction and ensures the fidelity of the transmitted quantum state. While quantum teleportation is advantageous for transmitting quantum information over long distances, LOCC protocols are particularly well-suited for applications like distributed quantum computing or quantum secret sharing that require joint operations on a shared entangled state [29].

G. Entanglement Enhancement

Applying LOCC to the W-state allows for entanglement distillation, potentially resulting in a final three-qubit state with a higher degree of entanglement or one tailored to fulfill specific entanglement-based purposes, such as secure quantum communication, QKD, or quantum teleportation. The connection between LOCC and W-states lies in the utilization of LOCC principles to manipulate and distill entanglement from a three-qubit W-state. Local operations and classical communication are integral to achieving specific entanglement-related goals, with W-states serving as the foundational resource. By performing local operations on their respective qubits and engaging in classical communication, multiple parties can collaboratively create and modify the W-state. This approach demonstrates the potential for LOCC protocols to significantly enhance and refine the entanglement properties of W-states, unlocking a wide range of applications in quantum information science and quantum networks.

VI. Conclusion

This research article thoroughly investigated the generation and properties of the tripartite perfect W-state using universally accessible gates in superconducting qubit circuits, with applications in quantum communication. Both simulation and experimental results demonstrated the W-state's superior entanglement and robustness against decoherence, addressing challenges in 5G and 6G networks. We introduced a novel QISS protocol utilizing LOCC and validated it through quantum state tomography (QST), with the IBM Eagle r3 processor achieving a fidelity of 0.82 ± 0.02 for the perfect W-state circuit and 0.55 ± 0.03 for the entire communication process. This work lays the foundation for secure and efficient 5G and 6G systems. The efficient use of local operations and the W-state's symmetry facilitate practical implementations in quantum communication and computing. This research establishes a groundwork for future exploration into scalable quantum networks and advanced quantum encryption techniques. The successful simulation and experimental validation highlight the potential of quantum technologies for secure and efficient data transmission in next-generation networks, marking a significant advancement in communication systems.

Acknowledgment

The authors acknowledge the IBM open-source quantum Qiskit — SDK and the SQC (ibm_osaka) lab facilities.

References

[1] W. Jiang and B. Han, “Evolution Toward Sixth-Generation (6G) Mobile Cellular Systems,” in *Cellular Communication Networks and Standards: The Evolution from 1G to 6G*, Cham: Springer Nature Switzerland, 2024, pp. 195–210.

[2] S. Yrjölä, M. Matinmikko-Blue, and P. Ahokangas, “The Evolution of Mobile Communications,” in *The Changing World of Mobile Communications: 5G, 6G and the Future of Digital Services*, Cham: Springer International Publishing, 2024, pp. 13–43.

[3] L. Nadeem *et al.*, “Integration of D2D, Network Slicing, and MEC in 5G Cellular Networks: Survey and Challenges,” *IEEE Access*, vol. 9, pp. 37590–37612, 2021.

[4] P. R. Singh, V. K. Singh, R. Yadav, and S. N. Chaurasia, “6G networks for artificial intelligence-enabled smart cities applications: A scoping review,” *Telemat. Inform. Rep.*, vol. 9, p. 100044, Mar. 2023, doi: 10.1016/j.teler.2023.100044.

[5] M. Z. Ali *et al.*, “Quantum for 6G communication: A perspective,” *IET Quantum Commun.*, vol. 4, no. 3, pp. 112–124, 2023.

[6] T. Shuminoski, T. Janevski, A. Risteski, and M. Bogdanoski, “Security and QoS framework for 5G and next generation mobile broadband networks,” in *IEEE EUROCON 2017 -17th International Conference on Smart Technologies*, Jul. 2017, pp. 104–109.

[7] M. Ghaderibaneh, C. Zhan, H. Gupta, and C. R. Ramakrishnan, “Efficient Quantum Network Communication Using Optimized Entanglement Swapping Trees,” *IEEE Trans. Quantum Eng.*, vol. 3, pp. 1–20, 2022.

[8] “IBM Quantum breaks the 100-qubit processor barrier,” IBM Research Blog. Accessed: Jul. 28, 2023. [Online]. Available: https://research.ibm.com/blog/127-qubit-quantum-processor-eagle

[9] E. Diamanti, H.-K. Lo, B. Qi, and Z. Yuan, “Practical challenges in quantum key distribution,” *Npj Quantum Inf.*, vol. 2, no. 1, Art. no. 1, Nov. 2016.

[10] Y.-A. Chen *et al.*, “An integrated space-to-ground quantum communication network over 4,600 kilometres,” *Nature*, vol. 589, no. 7841, Art. no. 7841, Jan. 2021.

[11] “Quantum Xchange Launches ‘Phio’ the First Commercial QKD Network for Quantum Communications in the U.S.,” QuantumXC. Accessed: Apr. 27, 2023. [Online]. Available: https://quantumxc.com/blog/quantum-launches-phio/

[12] “Toshiba’s leap in long-distance quantum communication,” Toshiba Quantum Technology. Accessed: May 30, 2024. [Online]. Available: https://www.toshiba.eu/quantum/news/toshiba-announces-breakthrough-in-long-distance-quantum-communication/

[13] “SK Telecom Unveils World’s First QRNG-Powered 5G Smartphone.” Accessed: Jun. 19, 2024. [Online]. Available: https://www.sktelecom.com/en/press/press_detail.do?idx=1385&currentPage=1&type=&keyword=

[14] W. Dür, “Multipartite entanglement that is robust against disposal of particles,” *Phys. Rev. A*, vol. 63, no. 2, p. 020303, Jan. 2001.

[15] M. K. Vijayan, A. P. Lund, and P. P. Rohde, “A robust W-state encoding for linear quantum optics,” *Quantum*, vol. 4, p. 303, Aug. 2020, doi: 10.22331/q-2020-08-03-303.

[16] X.-H. Zhang, X.-Y. Yan, Y.-Q. Wang, and L.-H. Gong, “Tripartite Layered Quantum Key Distribution Scheme with a Symmetrical Key Structure,” *Int. J. Theor. Phys.*, vol. 59, no. 2, pp. 562–573, Feb. 2020, doi: 10.1007/s10773-019-04349-4.

[17] H. J. Briegel, D. E. Browne, W. Dür, R. Raussendorf, and M. Van den Nest, “Measurement-based quantum computation,” *Nat. Phys.*, vol. 5, no. 1, Art. no. 1, Jan. 2009, doi: 10.1038/nphys1157.

[18] A. Khrennikov, “Roots of quantum computing supremacy: superposition, entanglement, or complementarity?,” *Eur. Phys. J. Spec. Top.*, vol. 230, no. 4, pp. 1053–1057, Jun. 2021.

[19] M. A. Khan, M. N. Aman, and B. Sikdar, “Beyond Bits: A Review of Quantum Embedding Techniques for Efficient Information Processing,” *IEEE Access*, vol. 12, pp. 46118–46137, 2024.

[20] T. M. Forcer, A. J. G. Hey, D. A. Ross, and P. G. R. Smith, “Superposition, Entanglement and Quantum Computation,” *Quantum Inf. Comput.*, vol. 2, no. 2, Art. no. 2, Feb. 2002.

[21] H. Singh, Arvind, and K. Dorai, “Evolution of tripartite entangled states in a decohering environment and their experimental protection using dynamical decoupling,” *Phys. Rev. A*, vol. 97, no. 2, p. 022302, Feb. 2018.

[22] S. Bravyi, O. Dial, J. M. Gambetta, D. Gil, and Z. Nazario, “The Future of Quantum Computing with Superconducting Qubits,” *J. Appl. Phys.*, vol. 132, no. 16, p. 160902, Oct. 2022, doi: 10.1063/5.0082975.

[23] A. Rai and G. S. Agarwal, “Possibility of coherent phenomena such as Bloch oscillations with single photons via W states,” *Phys. Rev. A*, vol. 79, no. 5, p. 053849, May 2009, doi: 10.1103/PhysRevA.79.053849.

[24] W. Dür, G. Vidal, and J. I. Cirac, “Three qubits can be entangled in two inequivalent ways,” *Phys. Rev. A*, vol. 62, no. 6, p. 062314, Nov. 2000, doi: 10.1103/PhysRevA.62.062314.

[25] G. Liu, I. George, and E. Chitambar, “The Round Complexity of Local Operations and Classical Communication (LOCC) in Random-Party Entanglement Distillation,” Mar. 30, 2023, *arXiv*: arXiv:2204.00781. doi: 10.48550/arXiv.2204.00781.

[26] R. S. Sutor, *Dancing with qubits : how quantum computing works and how it can change the world*. Birmingham, UK: Packt Publishing, Ltd. Birmingham, UK, 2019.

[27] W. K. Wootters and W. H. Zurek, “A single quantum cannot be cloned,” *Nature*, vol. 299, no. 5886, Art. no. 5886, Oct. 1982, doi: 10.1038/299802a0.

[28] Z. Li *et al.*, “Entanglement-Assisted Quantum Networks: Mechanics, Enabling Technologies, Challenges, and Research Directions,” *IEEE Commun. Surv. Tutor.*, vol. 25, no. 4, pp. 2133–2189, 2023, doi: 10.1109/COMST.2023.3294240.

[29] Y.-H. Yang, F. Gao, X. Wu, S.-J. Qin, H.-J. Zuo, and Q.-Y. Wen, “Quantum secret sharing via local operations and classical communication,” *Sci. Rep.*, vol. 5, no. 1, Art. no. 1, Nov. 2015, doi: 10.1038/srep16967.